

Supplementary Information

Ultra-small $\text{Ge}_{1-x}\text{Sn}_x$ quantum dots with visible photoluminescence

Richard J Alan Esteves,^a Shopan Hafiz,^b Denis O. Demchenko,^c Ümit Özgür,^b and Indika U. Arachchige^{a*}

^aDepartment of Chemistry, Virginia Commonwealth University, Richmond, Virginia 23284-2006, United States

^bDepartment of Electrical and Computer Engineering, Virginia Commonwealth University, Richmond, Virginia 23284-3072, United States

^cDepartment of Physics, Virginia Commonwealth University, Richmond, Virginia 23284-2000, United States

Corresponding author Email: iuarachchige@vcu.edu

Experimental Section

Materials

Germanium diiodide (99.99+ %) and tin dichloride (>99.9985 % Ultra-Dry), were purchased from Strem Chemicals and Alfa Aesar, respectively and stored in a N₂ glove box. N-butyllithium (BuLi) 1.6 M in hexane was purchased from Sigma Aldrich. Organic solvents such as, 1-octadecene (ODE, 90%), oleylamine (OLA, 80-90%), and Rhodamine 101 inner salt (99%) were purchased from Fisher Scientific. ACS grade solvents such as chloroform, toluene, carbon tetrachloride, and methanol were purchased from Acros. OLA and ODE were dried by heating at 120 °C under vacuum for one hour prior to storage in a N₂ glovebox. Methanol was dried over molecular sieves and toluene was dried over Na and both were distilled prior to use. Carbon tetrachloride was degassed by bubbling N₂ through it and was stored under inert conditions. *(Caution: n-butyllithium is highly pyrophoric and must be handled in air free conditions by properly trained personal. Carbon tetrachloride is highly toxic and its use should be minimized to limit exposure.)*

Synthesis of Ultra-Small (1-3 nm) Ge_{1-x}Sn_x Quantum Dots (QDs)

In a typical synthesis of 1-3 nm Ge_{1-x}Sn_x QDs, appropriate amounts of GeI₂ and SnCl₂, 0.6 mmol of metal total, were combined with 20 mL of OLA in a three neck flask inside a glovebox. This set up was sealed and transferred to a Schlenk line, and heated under vacuum to 115 °C to produce a homogeneous orange color solution. The reaction was purged with nitrogen and ramped up to 230 °C. At 230 °C, a reducing mixture was injected, which consisted of 0.5-0.9 mL of BuLi in 3.0 mL of ODE. The temperature dropped to ~210 °C upon injection, and the mixture was reheated to 300 °C within 10-14 min. The entire set up was then rapidly cooled with compressed air to < 100 °C to produce ultra-small Ge_{1-x}Sn_x QDs.

Synthesis of Larger, Polydisperse (5-20 nm) Ge_{1-x}Sn_x QDs

A set of larger, polydisperse Ge_{1-x}Sn_x QDs (5-20 nm) were produced for STEM/EDS analysis, using a synthetic procedure reported in the literature.¹ Briefly, 0.6 mmol of metal halides, GeI₂/SnCl₂, were heated in OLA at 115 °C to produce a homogeneous orange color solution. This mixture was heated to 230 °C and BuLi (1.1 molar eq. of halides) in ODE (3.0 mL) was swiftly injected. Then the reaction was heated to 300 °C and the growth stage was extended to 10 min at 300 °C to produce larger polydisperse (5-20 nm) alloy NCs. This ensures a similar nucleation process for both ultra –small and larger, polydisperse Ge_{1-x}Sn_x NCs.

Isolation and Purification of QDs

After the desired growth time, the temperature was dropped below 100 °C and the crude reaction mixture was mixed with 10 mL of freshly distilled toluene. Then, 60-90 mL of freshly distilled methanol was added, the resultant mixture was centrifuged for 5 min to obtain an orange color powder. The supernatant was discarded and the precipitate was twice purified by dispersing in toluene and subsequent precipitation with methanol.

Characterization of QDs

Powder X-ray diffraction (PXRD) measurements were performed with a PANalytical X'Pert PRO X-Ray diffractometer calibrated with Si standard and equipped with a Cu K α anode ($\lambda = 1.54 \text{ \AA}$). Purified QDs were deposited on to a low background sample holder and diffraction patterns were collected at 45 kV and 40 mA operating conditions. A Cary 6000i spectrophotometer (Agilent Technologies) was used for solution absorption measurements and solid state diffuse reflectance (DRA) with an internal DRA 2500 attachment. Solid sample measurements were performed by mixing the dry QDs in a BaSO₄ matrix prior to analysis. Elemental compositions

were recorded by energy dispersive spectroscopy (EDS). EDS data were obtained in a Hitachi FE-SEM Su-70 scanning electron microscope (SEM) operating at 20 KeV with an in-situ EDAX detector. Dried QDs were adhered to an aluminum stub with double sided carbon tape prior to analysis. The elemental compositions were determined by averaging the atomic percentages of Ge and Sn acquired from 5 individual spots per sample. X-ray photoelectron spectroscopy (XPS) analyses were performed with a Thermofisher ESCALAB 250 equipped with Al $\kappa\alpha$ source. Samples were prepared by pressing them into indium foil (Sigma Aldrich) which was adhered to an aluminum stub with conductive carbon tape. Low resolution transmission electron micrographs (TEM) were recorded using a Zeiss Libra 120 microscope operating at an accelerating voltage of 120 kV. High resolution TEM (HRTEM) analyses were performed on a JEOL 2000FX scanning transmission electron microscope with LaB₆ source operating at 200 kV. Scanning transmission electron microscopy (STEM) and HRTEM images were recorded on a FEI Titan 8300 microscope equipped with a Gatan 794 multiscan camera operating at 200 kV. TEM samples were prepared by drop casting ~5 μ L of NCs, dispersed in CCl₄, onto a carbon coated copper grids and evaporating the solvent. Photoluminescence (PL) studies were performed using a frequency doubled Ti:sapphire laser (385 nm wavelength, 150 fs pulse width, 160 kHz to 80 MHz repetition rate) as the excitation source. The detector was a liquid N₂ cooled charge coupled device (CCD) camera connected to a spectrometer. Samples were drop cast onto a clean Si substrate and dried and stored under nitrogen. Quantum yield measurements were performed on a Cary Eclipse fluorescence spectrophotometer (Agilent Technologies). Rhodamine 101 and Ge_{x-1}Sn_x QDs were dissolved in CHCl₃ and the concentrations were adjusted so that the optical densities were matched at the respective excitation energies. Annealing studies were performed in a quartz tube under high purity argon flow, in a Thermo-Scientific Lindenburg Blue M furnace. Raman spectra were

acquired using a Horiba LABram HR Evolution Confocal Raman Spectrometer equipped with a 532 nm laser with powder samples deposited on an aluminum substrate.

Theoretical Electronic Structure Calculations of QDs

Calculations were performed for $\text{Ge}_{1-x}\text{Sn}_x$ QDs with diameters of 2.1 nm and 2.7 nm, with dangling bonds passivated by hydrogen. Since hybrid functional structure relaxations are computationally demanding (and likely in this case unnecessary), lattice relaxations were performed using the generalized gradient approximation (GGA)² to the density functional theory, with forces minimized to 0.05 eV/Å or less. The electronic structure was calculated using tuned Heyd-Scuseria-Ernzerhof (HSE) hybrid functional calculations and the projector-augmented wave (PAW)³ formalism, as implemented in VASP,⁴ a plane-wave density functional code. In HSE hybrid functional, the semi-local Perdew-Burke-Ernzerhof exchange correlation part of the density functional is mixed with a Fock-type exchange in varying proportions at short range. In our calculations, the fraction of exact exchange was kept at a standard 25%, while the exchange range separation parameter was increased to 0.29 Å⁻¹, corresponding to the exchange screening length of 6.9 Å. The plane-wave basis sets with an energy cut-off of 250 eV were used. These parameters were found to reproduce bulk band structure of Ge in excellent agreement with experiment⁵ and as such, are expected to be consistent for $\text{Ge}_{1-x}\text{Sn}_x$ alloy QDs. Test calculations performed for pure Ge QDs compared with previously published results obtained using empirical pseudopotential calculations⁶ show that the bandgaps of QDs are accurately reproduced. Excitonic effects were calculated using time-dependent hybrid functional (TD-HSE) calculations.

X-Ray Photoelectron Spectroscopic Analysis of Ultra-Small Ge_{1-x}Sn_x QDs

The XPS spectra of ultra-small Ge_{1-x}Sn_x QDs are consistent with previous reports.^{1,7} The peaks observed in the Ge (3d) spectra at 30.0 eV and 32.5 eV can be assigned to Ge⁰ and Ge²⁺, respectively (Fig. S1). There is a noted absence of Ge⁴⁺ which would indicate GeO₂.^{1,7,8} The relative intensity of the two peaks suggests a large contribution from the surface of the QDs as is expected for ultra-small QDs with a large surface to volume ratio. Examination of the Sn (3d) region indicates a similar story, with both core Sn⁰ (486.9 eV) and surface Sn^{4+/2+} (488.8) present in the sample (Fig. S1).^{1,7,8} The Sn peaks are shifted to higher energies due to surface charging effect commonly observed in XPS analysis of nanoparticles.^{1,9} In combination with XRD, Raman, and STEM/ EDS maps, the presence of Sn⁰ confirms that SnCl₂ was successfully reduced and incorporated into the as-prepared Ge_{1-x}Sn_x QDs with no surface segregation. Both the Sn^{4+/2+} and Ge²⁺ peaks are attributed to surface atoms bound to stabilizing ligands, similar to a previous report.¹ The potential presence of SnO₂ is ruled out by a lack of a O (1s) peak at 530.6 eV.⁸ The O (1s) peaks observed at 531.9 and 534.1 eV are attributed to adsorbed H₂O and CO₂ from the atmosphere.

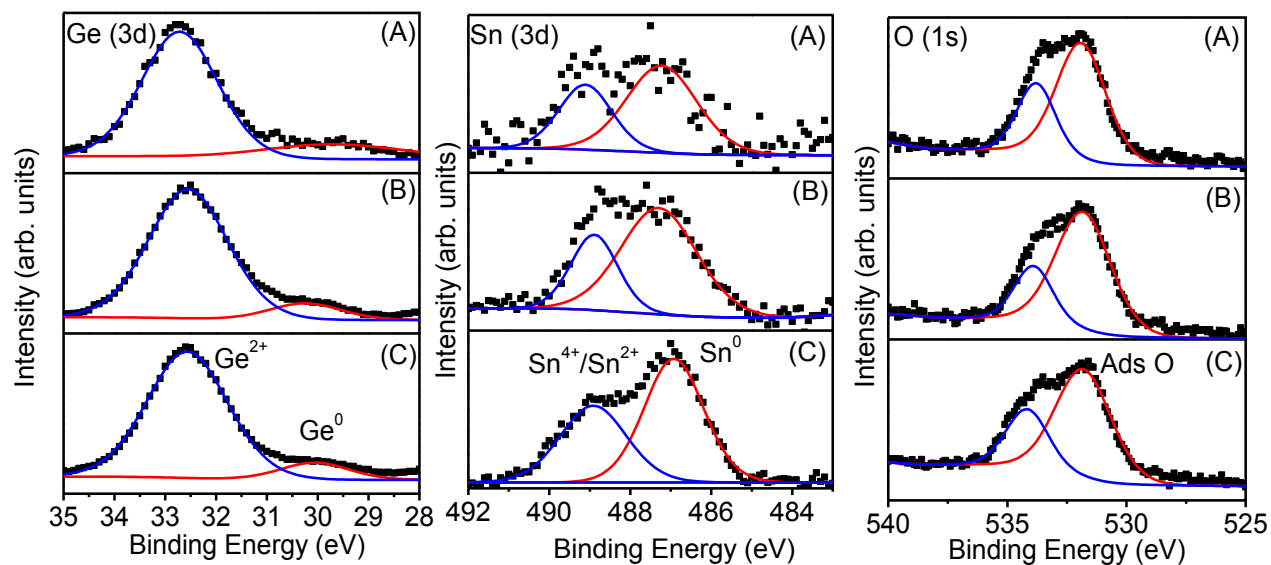


Fig. S1. Representative X-ray photoelectron spectra of ultra-small $\text{Ge}_{1-x}\text{Sn}_x$ QDs: (A) $x = 0.018$, (B) $x = 0.046$, (C) $x = 0.066$. Dotted lines represent spectral data and solid blue and red lines are fitted deconvolutions.

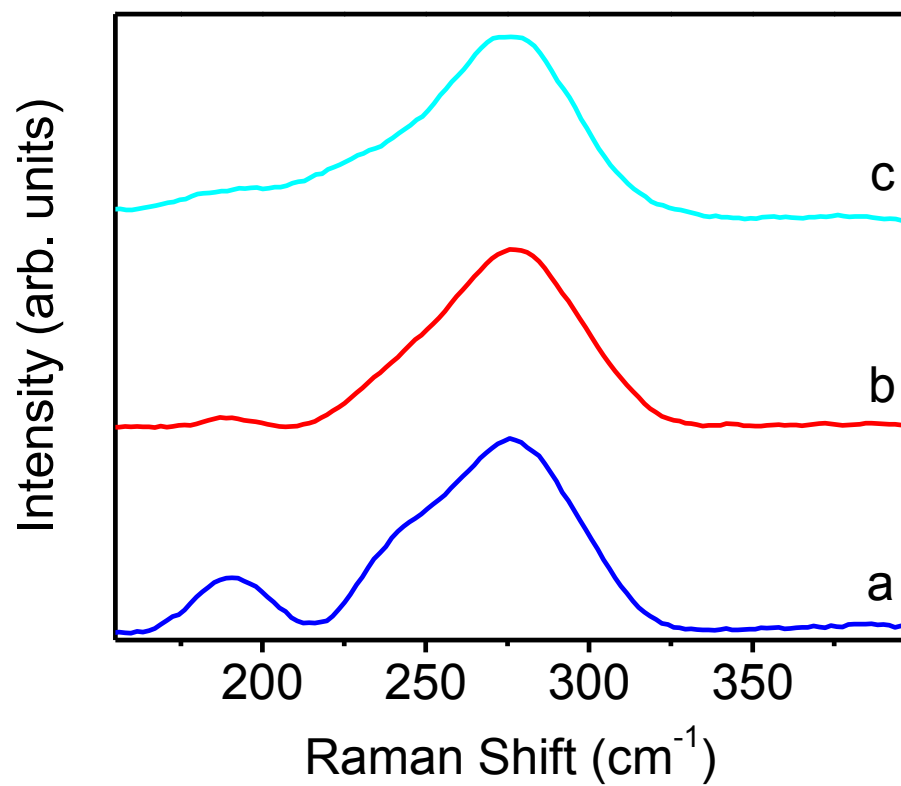


Fig. S2 Raman spectra of ultra-small Ge_{1-x}Sn_x QDs (1.85 ± 0.47 - 2.28 ± 0.48 nm) with varying Sn composition: $x =$ (a) 0.018, (b) 0.066, and (c) 0.236.

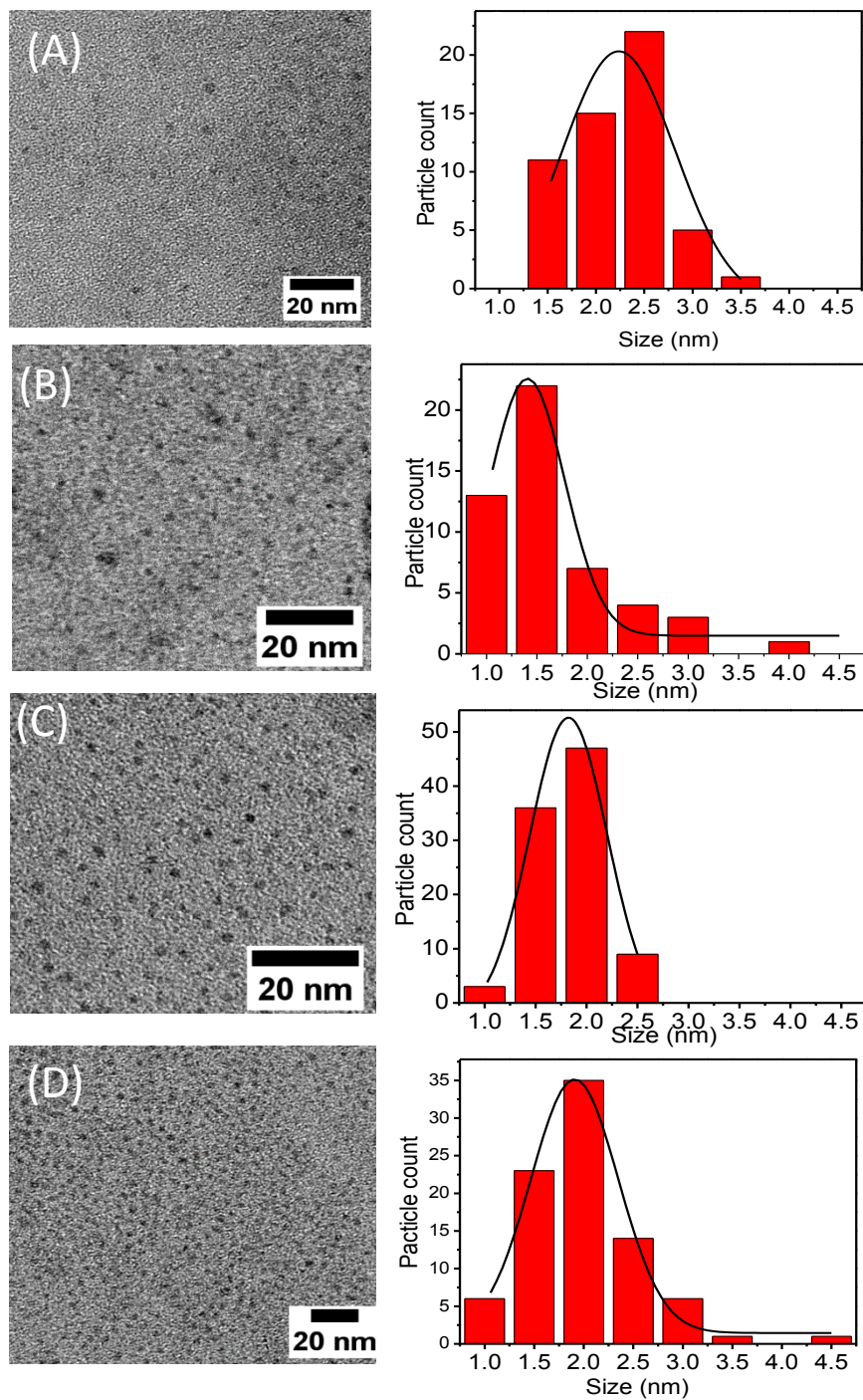


Fig. S3 Bright field TEM images of ultra-small Ge_{1-x}Sn_x QDs with varying Sn composition: (A) $x = 0.018$, (B) $x = 0.046$, (C) $x = 0.066$, and (D) $x = 0.236$. The corresponding size histograms of Ge_{1-x}Sn_x QDs without any post-synthetic size selection are also shown.

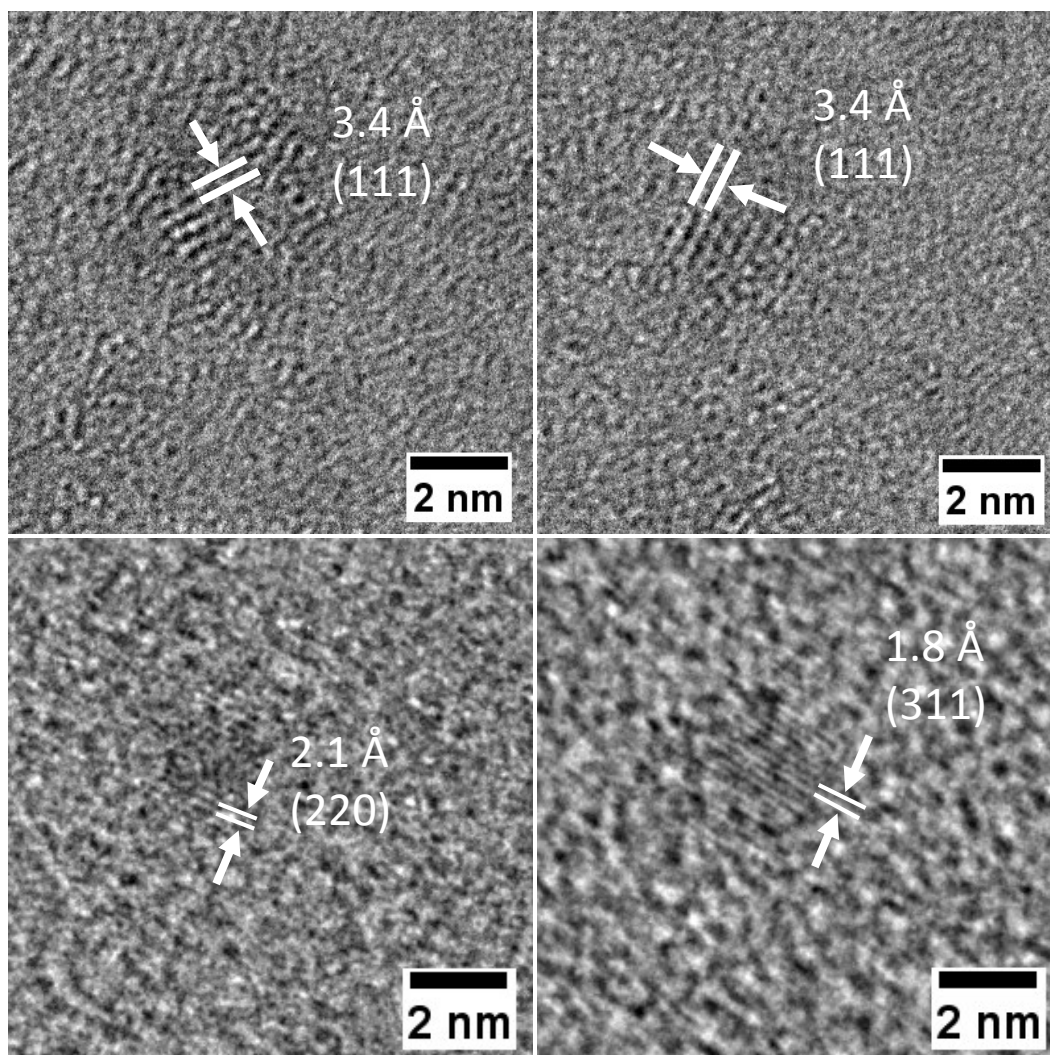


Fig. S4 High resolution TEM images of $2.0 \pm 0.57 \text{ nm}$ $\text{Ge}_{0.764}\text{Sn}_{0.236}$ QDs. Visible lattice fringes are measured at 3.4 , 2.1 , and 1.8 \AA corresponds to expanded (111), (220), and (311) planes of diamond cubic $\text{Ge}_{1-x}\text{Sn}_x$.

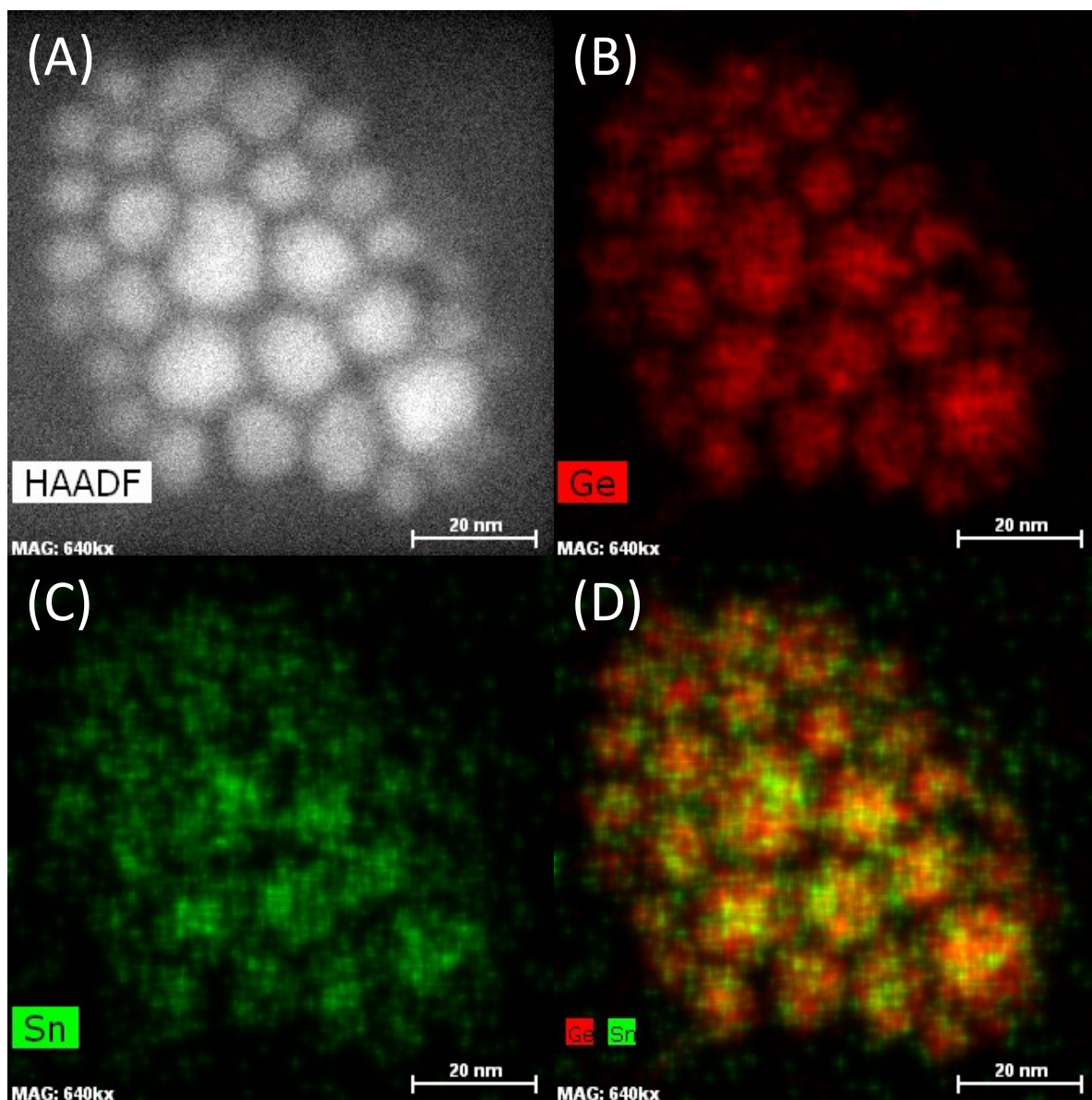


Fig. S5 (A) Dark field TEM image of a polydisperse mixture of larger Ge_{0.87}Sn_{0.23} NCs (5-20 nm) along with STEM/EDS elemental maps of (B) Ge, (C) Sn, and (D) an overlay of Ge and Sn indicating the homogeneous distribution of elemental components throughout the lattice.

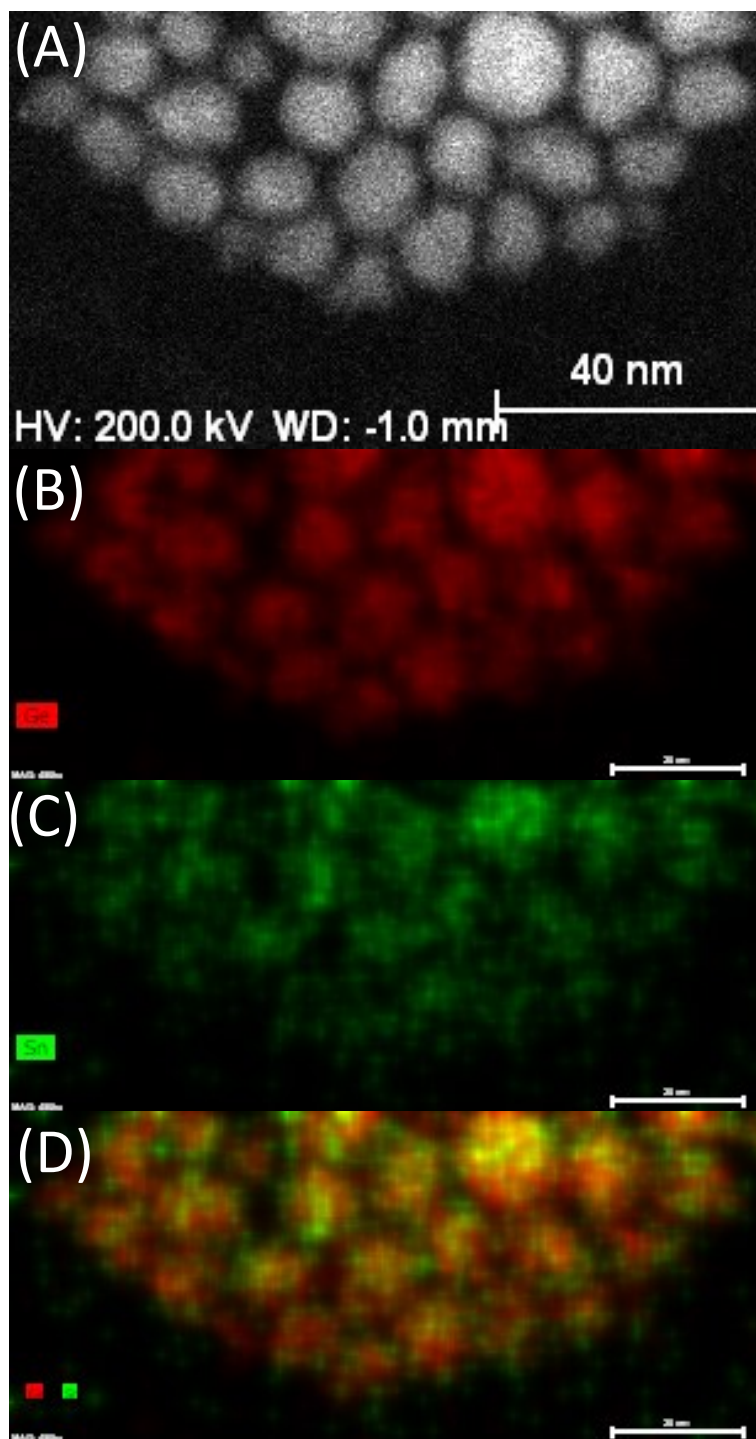


Fig. S6 (A) Dark filed TEM image of a polydisperse mixture of larger Ge_{0.87}Sn_{0.23} NCs (5-20 nm) along with STEM/EDS elemental maps of (B) Ge, (C) Sn, and (D) an overlay of Ge and Sn indicating the homogeneous distribution of elemental components in this size regime.

Table S1. Elemental composition of ultra-small Ge_{1-x}Sn_x QDs acquired from energy dispersive spectroscopy (EDS) and X-ray photoelectron spectroscopy (XPS) analyses.

Sample	Sn composition from EDS ^a	Sn composition XPS ^b
Ge _{1-x} Sn _x	0.018 ± 0.07	0.0184
Ge _{1-x} Sn _x	0.046 ± 1.2	0.0479
Ge _{1-x} Sn _x	0.066 ± 0.5	0.075
Ge _{1-x} Sn _x	0.236 ± 1.4	N/A

^aSn compositions were obtained in terms of atomic % from SEM/EDS, and averaging five individual measurements per each sample. ^bSn compositions were obtained from the ratio of Ge(3d) and Sn(3d) in XPS calculated with atomic sensitivity factors of 0.38 and 4.30, respectively.⁸

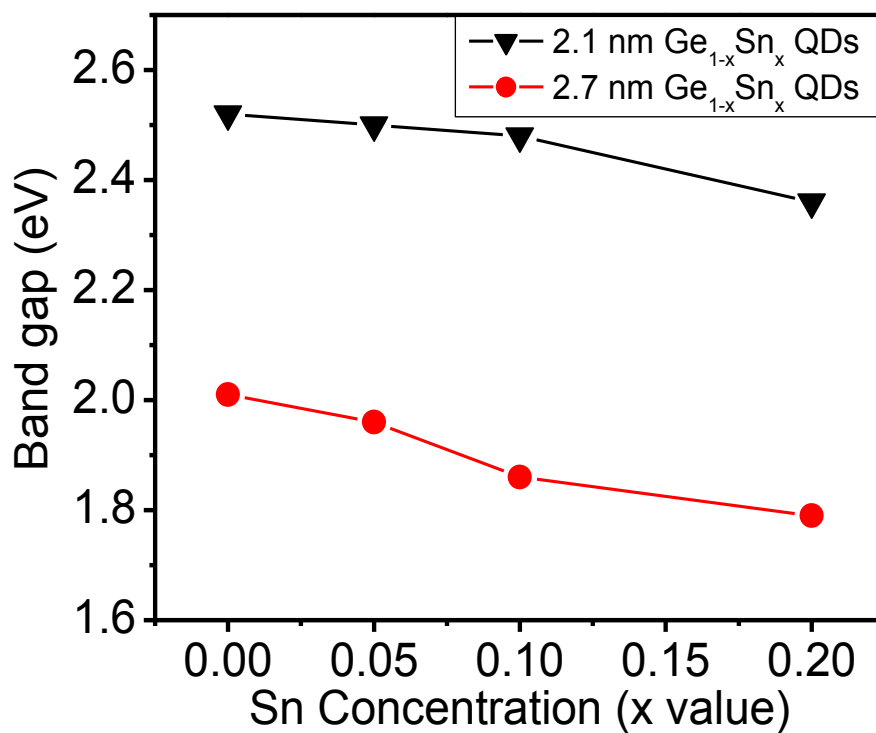


Fig. S7. Theoretical energy gaps of 2.1 nm and 2.7 nm $\text{Ge}_{1-x}\text{Sn}_x$ QDs with varying Sn composition calculated using tuned Heyd-Scuseria-Ernzerhof hybrid functional calculations.

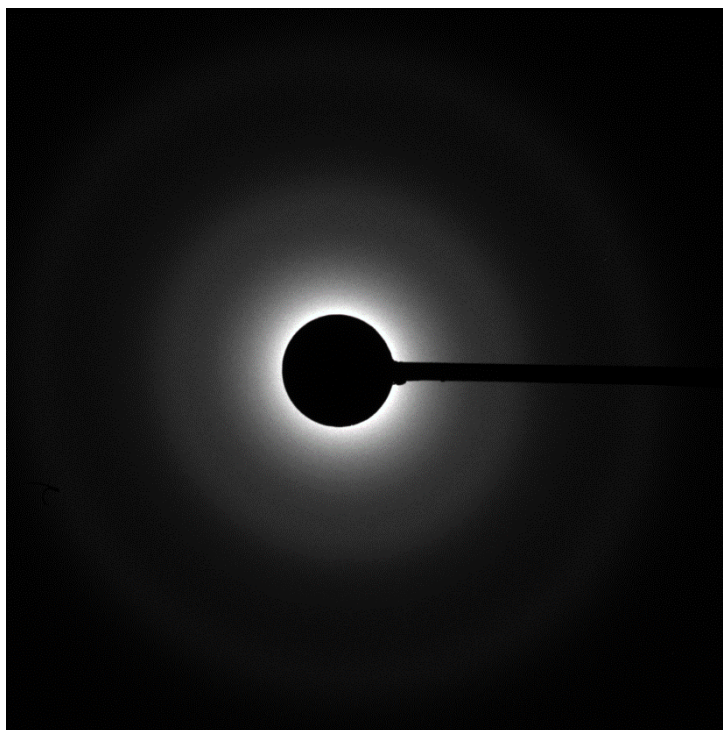


Fig. S8. Representative electron diffraction pattern of ultra-small $\text{Ge}_{0.934}\text{Sn}_{0.066}$ QDs.

References

1. R. J. Esteves, M. Q. Ho and I. U. Arachchige, *Chem. Mater.*, 2015, **27**, 1559.
2. J. P. Perdew, *Phys. Rev. Lett.*, 1985, **55**, 1665.
3. P. E. Blöchl, *Phys. Rev. B*, 1994, **50**, 17953.
4. G. Kresse and J. Furthmüller, *Phys. Rev. B*, 1996, **54**, 11169.
5. M. Levinstein, S. Rumyantsev, M. Shur, *Handbook Series on Semiconductor Parameters* vol. 1, 2 edited, World Scientific, London, 1999.
6. F.A. Reboredo and A. Zunger, *Phys. Rev. B*, 2000, **62**, R2275.
7. K. Ramasamy, P. G. Kotula, A. F. Fidler, M. T. Brumbach, J. M. Pietryga and S. A. Ivanov, *Chem. Mater.*, 2015, **27**, 4640.
8. D. Briggs, M. P. Seah, *Practical Surface Science 2nd Ed.*, vol. 1, 2 John Wiley & Sons, Great Britain, 1948.
9. K. K Kalebaila, D. G. Georgiev, S. L. Brock, *J. Non-Cryst. Solids*, 2006, **352**, 232.